

<Supporting Information>

Trinuclear ruthenium core-containing polyoxometalate-based hybrids: Preparation, Characterization and Catalysis Behavior

Huafeng Li, Peipei He, Rong Wan, Yan Zou, Xue Zhao, Pengtao Ma, Jingyang Niu* and Jingping Wang*

Henan Key Laboratory of Polyoxometalate Chemistry, College of Chemistry and Chemical Engineering, Henan University, Kaifeng, Henan 475004, China

Figure S1 a) Combined polyhedral/ball-and-stick representation of polyanion for **1**. b) Combined polyhedral/ball-and-stick representation of polyanion for analogue.

Figure S2 a) Combined polyhedral/ball-and-stick representation of polyanion for **2**. b) Polyhedral/ball-and-stick representation of $[\alpha\text{-AsW}_9\text{O}_{33}]^{9-}$ fragment. c) Polyhedral representation of their WO_5 fragments for **2**.

Figure S3 a) Polyhedral/ball-and-stick representation of compound **1**. b) Ball-and-stick representation of compound **1**.

Figure S4 a) Polyhedral/ball-and-stick representation of compound **2**. b) Ball-and-stick representation of compound **2**.

Figure S5 Negative mode ESI-MS of **2** and zoomed figure of peaks centered m/z 1023.14 and 1278.96, the simulated spectrum is shown in blue.

Figure S6 The ESI-MS spectrum of the catalyst **1** after three-run.

Figure S7 The thermogravimetric curves of compounds **1** and **2**.

Figure S8 Positive mode ESI-MS of **1** and **2**.

Table S1 Selected bond distances of compounds **1** and **2**.

Table S2 Selected bond angles of compounds **1** and **2**.

Table S3 BVS values of As, W and Ru atoms in **1**.

Table S4 BVS values of As, W and Ru atoms in **2**.

Table S5 Crystal data and structure refinements of compounds **1** and **2**.

Table S6 The thermogravimetric analyses of compounds **1** and **2**.

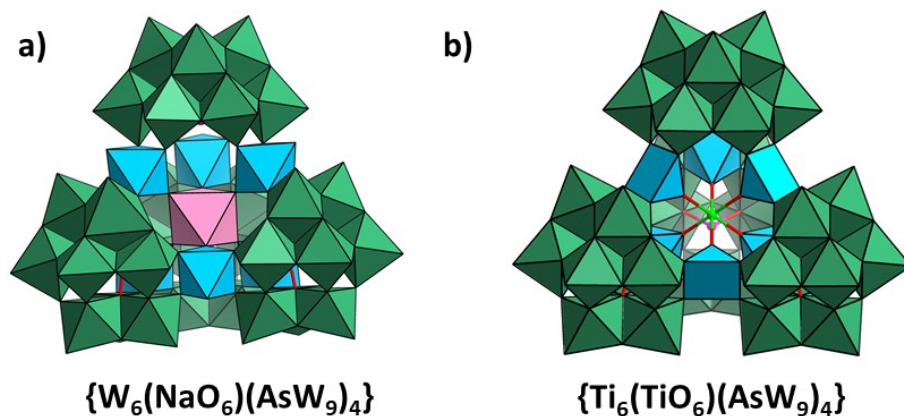


Figure S1. a) Combined polyhedral/ball-and-stick representation of polyanion for **1**. b) Combined polyhedral/ball-and-stick representation of polyanion for analogue. Color code: As (pink), Ti (bright green), NaO₆ octahedra (rose), WO₆ octahedra (sea green), bridging group WO₆ octahedron (sky blue) and TiO₅ pentahedron (blue); all hydrogen atoms have been omitted for clarity.

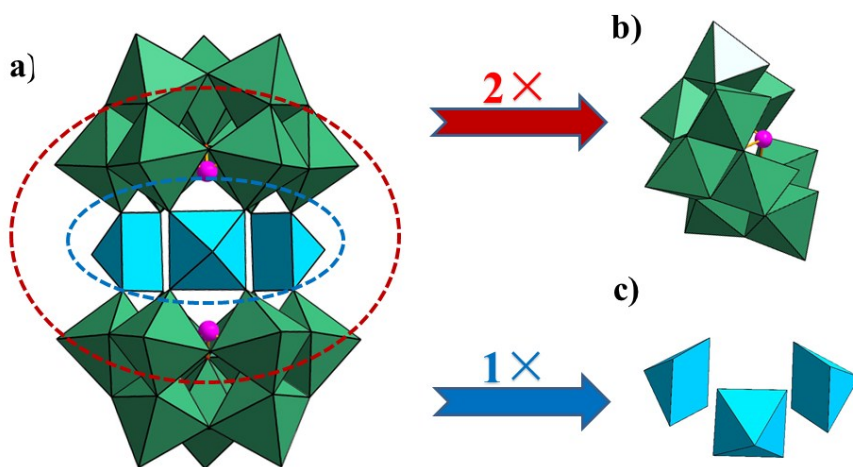


Figure S2. a) Combined polyhedral/ball-and-stick representation of polyanion for **2**. b) Polyhedral/ball-and-stick representation of [α -AsW₉O₃₃]⁹⁻ fragment. c) Polyhedral representation of three WO₅ fragments for **2**. Color code: As (pink), WO₆ octahedra (sea green) and bridging group WO₅ square-pyramidally (sky blue); all hydrogen atoms have been omitted for clarity.

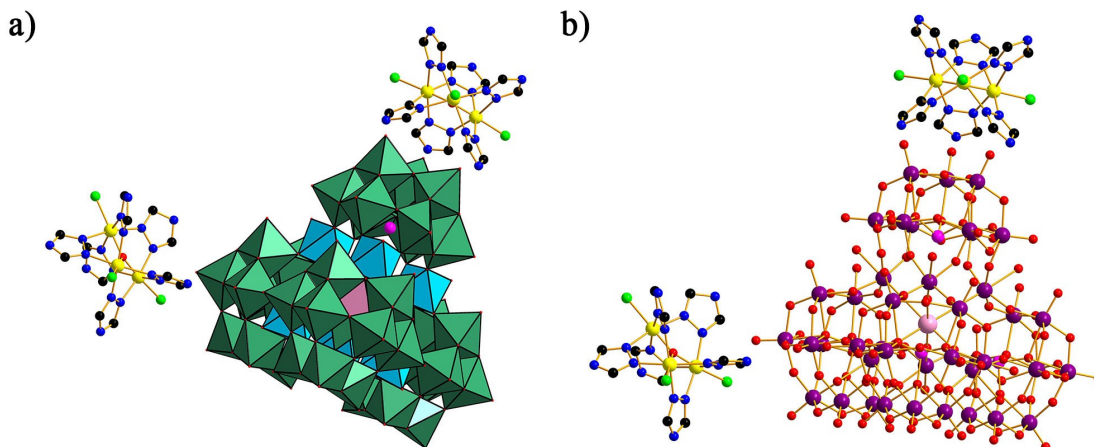


Figure S3. a) Polyhedral/ball-and-stick representation of compound **1**. b) Ball-and-stick representation of compound **1**. Color code: C (black), N (blue), O (red), Cl (bright green), Ru (yellow), As (pink), W (violet), Na (gray), NaO₆(rose), WO₆ octahedra (sea green) and bridging group WO₆ octahedron (sky blue); all hydrogen atoms have been omitted for clarity.

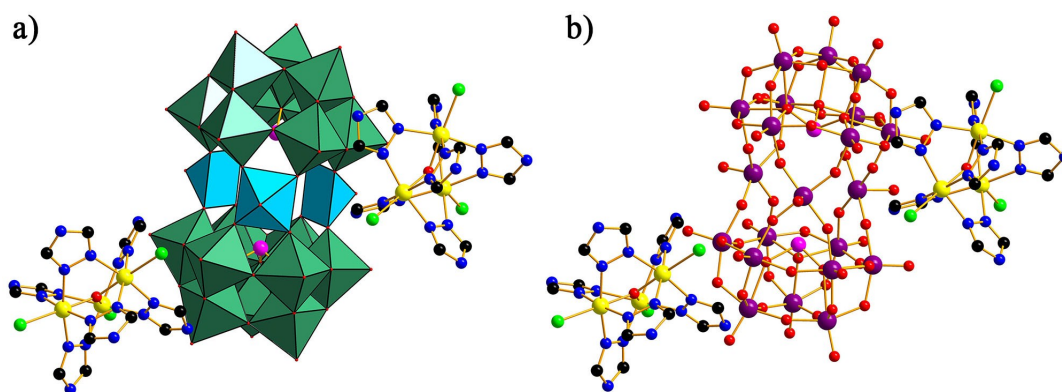


Figure S4. a) Polyhedral/ball-and-stick representation of compound **2**. b) Ball-and-stick representation of compound **2**. Color code: C (black), N (blue), O (red), Cl (bright green), Ru (yellow), As (pink), W (violet), WO₆ octahedra (sea green) and bridging group WO₅ square-pyramidally (sky blue); all hydrogen atoms have been omitted for clarity.

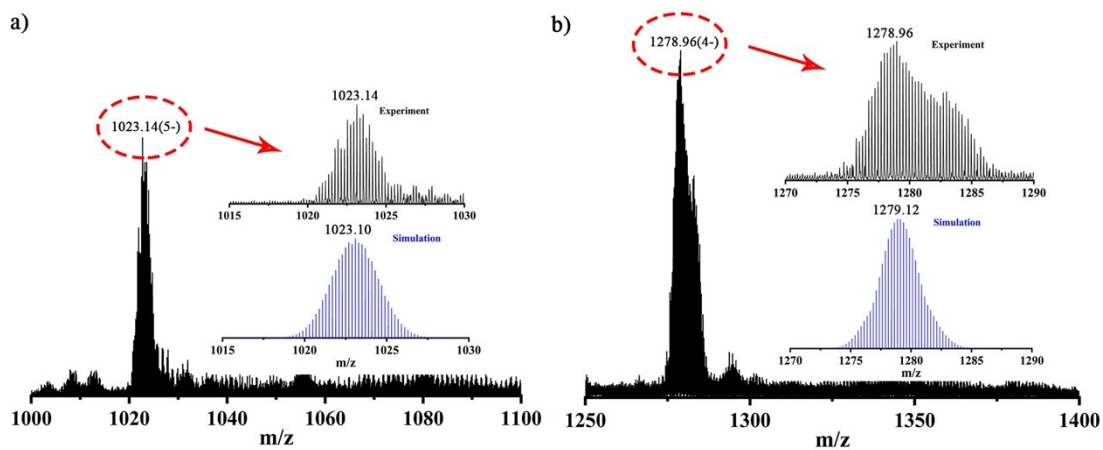


Figure S5. Negative mode ESI-MS of 2 and zoomed figure of peaks centered m/z 1023.14 and 1278.96, the simulated spectrum is shown in blue.

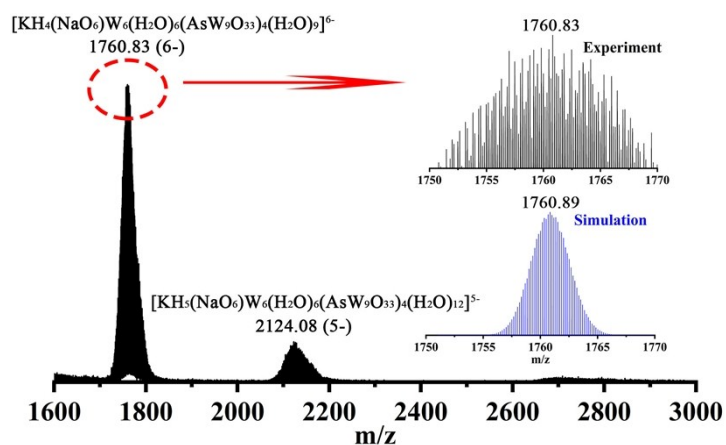


Figure S6. The ESI-MS spectrum of the catalyst 1 after five-run.

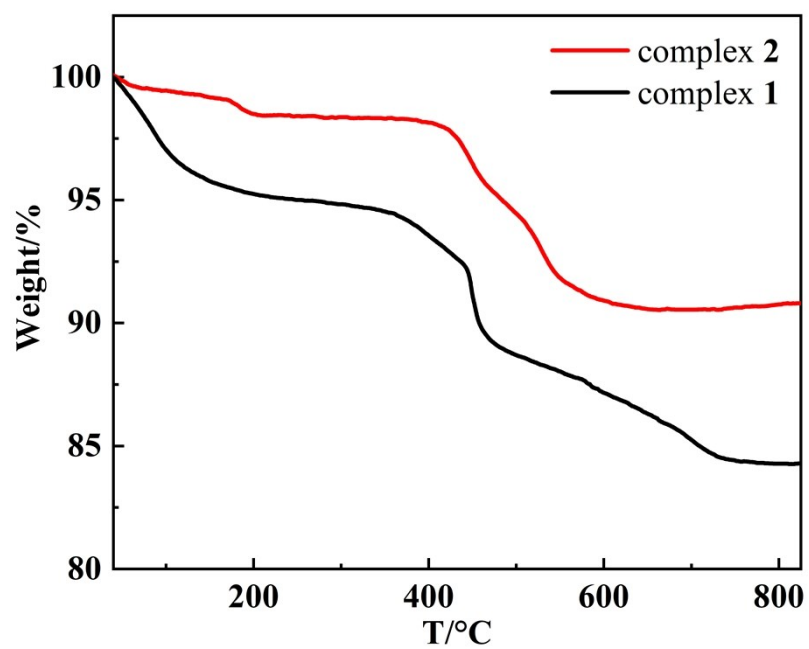


Figure S7. The thermogravimetric curves of 1 and 2.

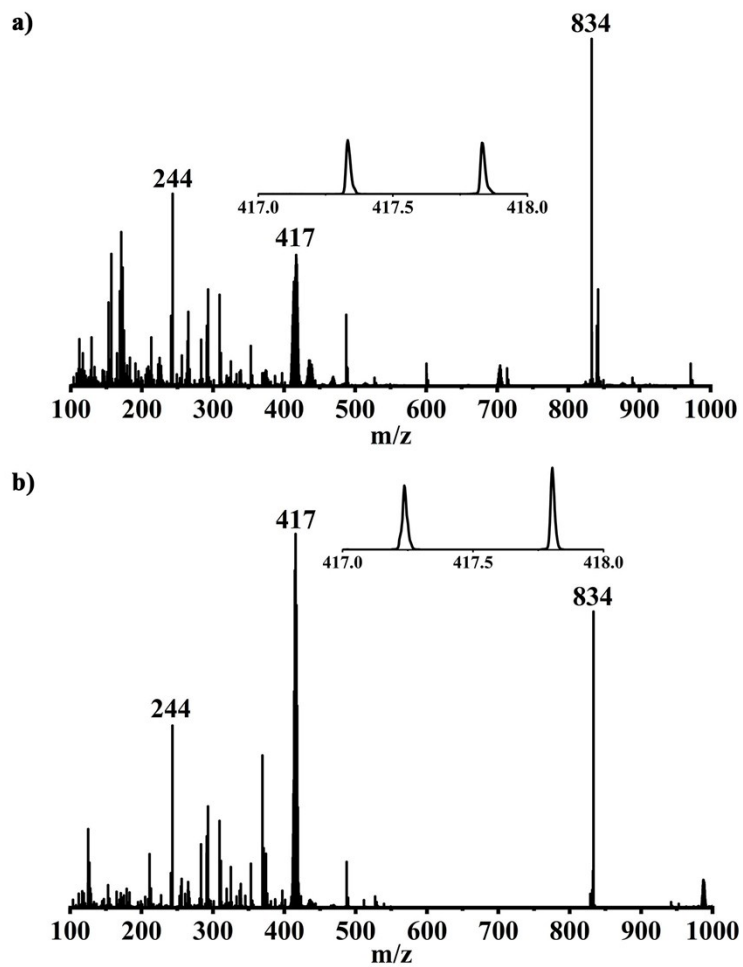


Figure S8 Positive mode ESI-MS of 1 and 2.

Table S1. Selected bond distances of compounds **1** and **2**.

	1		2
Ru1–O146	1.88 (2)	Ru1–O34	1.855 (12)
Ru1–N1	2.01 (3)	Ru1–N1	2.04 (2)
Ru1–N10	2.07 (3)	Ru1–N5 ²	2.04 (2)
Ru1–N12	2.01 (3)	Ru1–N7	2.073 (19)
Ru1–N15	2.05 (3)	Ru1–N9	2.05 (2)
Ru1–C11	2.383 (9)	Ru1–C11	2.393 (8)
Ru2–O146	1.86 (2)	Ru2–O34	1.90 (2)
Ru2–N5	2.08 (3)	Ru2–N3 ²	2.081 (18)
Ru2–N7	2.08 (3)	Ru2–N3	2.081 (18)
Ru2–N14	2.05 (2)	Ru2–N4	2.090 (17)
Ru2–N36	1.95 (3)	Ru2–N4 ²	2.090 (17)
Ru2–Cl2	2.376 (10)	Ru2–Cl2	2.371 (13)
Ru3–O146	1.87 (2)	Ru3–O38	1.87 (2)
Ru3–N2	2.08 (3)	Ru3–N12	2.062 (19)
Ru3–N4	2.02 (3)	Ru3–N12 ¹	2.062 (19)
Ru3–N6	2.06 (3)	Ru3–N14 ¹	2.09 (2)
Ru3–N9	2.07 (2)	Ru3–N14	2.09 (2)
Ru3–Cl3	2.362 (10)	Ru3–Cl4	2.378 (12)

Table S2. Selected bond angles of compounds **1** and **2**.

1		2	
O146-Ru1-C11	178.5 (7)	O34-Ru1-C11	179.8 (6)
O146-Ru1-N1	84.7 (11)	O34-Ru1-N1	86.7 (9)
O146-Ru1-N10	85.0 (10)	O34-Ru1-N52	86.3 (9)
O146-Ru1-N12	85.1 (11)	O34-Ru1-N7	83.4 (8)
O146-Ru1-N15	83.2 (11)	O34-Ru1-N9	84.8 (10)
N1-Ru1-C11	95.6 (9)	N1-Ru1-C11	93.6 (7)
N1-Ru1-N10	81.6 (10)	N1-Ru1-N52	83.8 (8)
N1-Ru1-N12	169.5 (12)	N1-Ru1-N7	170.0 (8)
N1-Ru1-N15	94.9 (11)	N1-Ru1-N9	97.6 (8)
N10-Ru1-C11	93.5 (8)	N52-Ru1-C11	93.7 (6)
N12-Ru1- C11	94.5 (9)	N52-Ru1-N9	170.9 (9)
N12-Ru1-N10	95.2 (10)	N7-Ru1-C11	96.4 (6)
N12-Ru1- N15	86.2 (11)	N7-Ru1-N52	95.0 (8)
N15-Ru1-C11	98.3 (9)	N7-Ru1-N9	82.1 (8)
N15-Ru1-N10	168.0 (11)	N9-Ru1-C11	95.3 (7)
O146-Ru1-C11	178.5 (7)	O34-Ru1-C11	179.8 (6)
O146-Ru1-N1	84.7 (11)	O34-Ru1-N1	86.7 (9)
O146-Ru1-N10	85.0 (10)	O34-Ru1-N52	86.3 (9)

Table S3. BVS values of Ru, As, W and selected O atoms of compound 1.

Atom	BVS	Atom	BVS	Atom	BVS	Atom	BVS
Ru1	3.752	Ru2	3.802	Ru3	3.680	Ru4	3.570
Ru5	3.638	Ru6	3.858	As1	3.079	As2	2.940
As3	2.967	As4	2.971	W1	6.336	W2	6.150
W3	5.981	W4	6.080	W5	6.306	W6	5.981
W7	6.072	W8	6.242	W9	6.086	W10	6.232
W11	6.161	W12	6.314	W13	5.912	W14	5.857
W15	6.691	W16	6.012	W17	6.238	W18	6.196
W19	6.054	W20	5.880	W21	5.943	W22	6.412
W23	6.182	W24	6.066	W25	6.107	W26	6.263
W27	6.011	W28	6.356	W29	6.216	W30	6.242
W31	5.864	W32	6.260	W33	6.104	W34	6.594
W35	6.639	W36	5.827	W37	5.899	W38	6.004
W39	6.361	W40	6.326	W41	6.322	W42	5.944
O146	-2.290	O147	-2.322	O50	-0.213	O115	-0.264
O120	-0.278	O130	-0.243	O137	-0.310	O140	-0.286

Table S4. BVS values of Ru, As, W and selected O atoms of compound 2.

Atom	BVS	Atom	BVS	Atom	BVS	Atom	BVS
Ru1	3.696	Ru 2	3.810	Ru3	3.781	As1	3.076
W1	5.987	W2	6.170	W3	6.066	W4	6.257
W5	6.225	W6	6.018	W7	5.503	W8	6.121
W9	6.212	W10	6.423	W11	6.332	W12	6.010
O25	-2.058	O34	-2.293	O38	-2.273	O39	-0.832

Table S5. Crystal Data and Structure Refinements for compounds **1** and **2**.

Compound	1	2
Empirical Formula	C ₂₄ H ₁₀₀ N ₃₆ Ru ₆ Cl ₆ KNaAs ₄ W ₄₂ O ₁₇₄	C ₂₄ H ₄₀ N ₃₆ Ru ₆ Cl ₆ As ₂ W ₂₁ O ₇₇
Formula weight (g mol ⁻¹)	12579.38	6894.39
λ (Å)	0.71073	0.71073
<i>T</i> (K)	150(1)	150(1)
Crystal system	Triclinic	Monoclinic
Space group	<i>P</i> -1	<i>P</i> 2 ₁ / <i>m</i>
<i>a</i> (Å)	20.0498(11)	18.3691(5)
<i>b</i> (Å)	24.3323(11)	18.3890(6)
<i>c</i> (Å)	25.4119(12)	22.2929(6)
α (deg)	89.231(2)	90
β (deg)	72.661(2)	108.3577(12)
γ (deg)	80.351(2)	90
Volume (Å ³)	11657.8(10)	7147.1(4)
<i>Z</i>	2	2
<i>D</i> _{calc} (g cm ⁻³)	3.474	3.195
μ (mm ⁻¹)	21.739	18.089
Limiting indices	-23 ≤ <i>h</i> ≤ 23 -29 ≤ <i>k</i> ≤ 29 -30 ≤ <i>l</i> ≤ 29	-21 ≤ <i>h</i> ≤ 21 -21 ≤ <i>k</i> ≤ 21, -26 ≤ <i>l</i> ≤ 26
Reflns collected	171590	71079
<i>R</i> _{int}	0.0686	0.0789
Goodness-of-fit on <i>F</i> ²	1.134	1.025
<i>R</i> _{<i>I</i>} ^{<i>a</i>} [<i>I</i> > 2σ (<i>I</i>)]	0.1042	0.0735
<i>wR</i> ₂ ^{<i>b</i>} [<i>I</i> > 2σ (<i>I</i>)]	0.2754	0.1913
<i>R</i> _{<i>I</i>} ^{<i>a</i>} [all data]	0.1335	0.0983
<i>wR</i> ₂ ^{<i>b</i>} [all data]	0.3173	0.2175

^a $R_1 = \sum |F_o| - |F_c| / \sum |F_o|$. ^b $wR_2 = \{ \sum [w(F_o^2 - F_c^2)^2] / \sum [w(F_o^2)^2] \}^{1/2}$.

Table S6. The thermogravimetric analyses of compounds **1** and **2**.

Compound	Theoretical (two steps, %)	Experimental (two steps, %)
1	4.87, 10.48	4.96, 10.50
2	1.57, 7.77	1.62, 7.91

Thermogravimetric Analyses.

As shown in Figure S7, the thermal stability of compounds **1** and **2** have been determined by using thermogravimetric analyses. The thermogravimetric curves are very similar and show two major weight loss stages in the region of 50–825 °C. Hence, only the thermogravimetric curve of **1** is taken as a representative to describe in detail. For **1**, the observed total weight loss (15.46 %) is agreement with the calculated value (15.35 %). The first weight loss of 4.96 % from 50 to 300 °C was due to the release of twenty-eight lattice water molecules and six coordinated water ligands (calcd 4.87 %). The last weight loss of 10.50 % from 300 to 825 °C was corresponded to the removal of two As₂O₃ molecules and twelve ligands (calcd 10.48 %). The first weight loss is more than the theoretical value, which may be ascribed to the fact that the samples have been weathered before the thermogravimetric analyses. The similar process of thermogravimetric analyses of compound **2** is shown in Table S6.